

Dielectric tunable characteristics of compositional-gradient BaTi_{1-x}Sn_xO₃ thin films

Chenjing Wu and Manwen Yao*

Functional Materials Research Laboratory
School of Materials Science & Engineering
Tongji University, No. 4800 Cao'an Road
Shanghai 201804, P. R. China

*yaomw@tongji.edu.cn

Received 20 April 2021; Accepted 21 June 2021; Published 6 September 2021

Compositional-gradient BaTi_{1-x}Sn_xO₃ thin films on Pt(100)/Ti/SiO₂/Si substrates are fabricated with sol-gel using spin coating. All of the structures of the prepared thin films are of single-phase crystalline perovskite with a dense and crack-free surface morphology. BTS10/15/20 thin film exhibits enhanced temperature stability in its dielectric behavior. The temperature coefficient of capacitance TCC₂₀₋₁₅₀ in the temperature range from 20 °C to 150 °C is $-0.9 \times 10^{-4}/^{\circ}\text{C}$ and that of TCC_{20-(-95)}} in the temperature range from 20 °C to -95 °C is $-3.8 \times 10^{-4}/^{\circ}\text{C}$. Furthermore, the thin films show low leakage current density and dielectric loss. High and stable dielectric tunable performances are found in BTS10/15/20 thin films: the dielectric tunability of the thin films is around 20.1% under a bias voltage of 8 V at 1 MHz and the corresponding dielectric constant is in the range between 89 and 111, which is beneficial for impedance matching in circuits. Dielectric tunability can be obtained under a low tuning voltage, which helps ensure safety. The simulated resonant frequency of the compositional-gradient BTS thin films depends on the bias electric field, showing compositional-gradient BTS thin films could be used in electrically tunable components and devices. These properties make compositional-gradient BTS thin films a promising candidate for dielectric tuning.

Keywords: Barium stannate titanate; compositional-gradient thin films; dielectric tunable performance; temperature stability.

1. Introduction

Nonlinear dielectric materials have attracted much attention, as they can be used with a variety of electrically tunable components and devices, such as phase shifters, tunable filters, delay lines, tunable antennas, and oscillators.¹⁻⁵ Tunable antennas, for example, can control the frequency and/or direction of power radiation in their operation.⁶ It is important to recognize electrically tunable applications and obtain high-quality performance. Electrically tunable applications can be achieved with dielectric nonlinearity, that is, nonlinear polarization under a bias electric field.⁷ This does not require coils or complex circuits, and can also support the miniaturization of electronic components and devices. For these reasons, nonlinear dielectric materials have become a research hotspot in recent years.⁸⁻¹²

When nonlinear dielectric materials are used with electrically tunable components and devices, it is required to have great temperature stability, high dielectric tunability, a moderate dielectric constant, low dielectric loss, and a high figure of merit (FOM).¹³ Dielectric tunability is a critical parameter, that represents the ability of the dielectric constant to vary with the bias electric field.

where $\epsilon(0)$ and $\epsilon(E)$ are the dielectric constant under a zero-bias electric field and under a certain applied bias electric field. From Eq. (1), it can be seen that tunability directly depends on dielectric constant, making the dielectric constant an obviously important parameter. According to Richtmyer, the size of the resonator is proportional to the reciprocal of the square root of the dielectric constant.¹⁴ That is, the larger the dielectric constant of the dielectric materials, the smaller the theoretical design size of the components and devices. However, larger dielectric constants are not always better due to the impedance mismatching in circuits and slow response of the circuit signal.¹⁵ Hence, taking both dielectric tunability and impedance matching into consideration, it is necessary to achieve a moderate dielectric constant. Another important parameter is dielectric loss, which can have negative effects on electrically tunable components and devices. It is only by reducing dielectric loss that application frequency can be increased. Hence, it is important to reduce dielectric loss as much as possible.¹⁶

For these three parameters, usually only one or two can be maintained at a high level, and not all parameters can reach an optimal state at the same time. For this reason, the FOM is introduced to comprehensively evaluate the performance of nonlinear dielectric materials.¹⁷

$$\text{Tunability} = (\epsilon(0) - \epsilon(E)) / \epsilon(0), \quad (1)$$

$$\text{FOM} = \text{Tunability} / \text{Dielectric Loss}. \quad (2)$$

*Corresponding author.

Barium titanate (BaTiO_3) has been studied widely due to its nonlinear dielectric properties and is a pillar of the electronic ceramic industry. It is environmentally friendly and nontoxic.^{18–20} It has become the most basic and widely used material in modern electronic ceramic components and devices. However, its high dielectric constant of BaTiO_3 can cause impedance mismatching in circuits, and high dielectric loss can limit the application frequency, as described above. To dilute the ferroelectricity of BaTiO_3 , which in turn can reduce the dielectric constant and dielectric loss, Sn-doped BaTiO_3 is employed.^{21,22} Barium stannate titanate ($\text{BaTi}_{1-x}\text{Sn}_x\text{O}_3$, BTS) possesses strong dielectric nonlinearity and low dielectric loss. When the doping ratio of Sn is appropriate, the dielectric constant can be adjusted to a moderate level while maintaining a high tunability. These excellent properties make BTS a powerful candidate for tunable components and devices, and this leads to broad application prospects. However, to achieve a high tunability of BTS ceramics, high tuning voltages must be applied, which entails a vulnerability to breakdown during operation. Therefore, BTS thin films are promising candidates for use in electrically tunable components and devices in relation to their low tuning voltage and miniaturization.

Recently, a range of compositional modifications and architectural designs have been proposed to improve the dielectric properties of thin films. Compositional-gradient thin films have been developed that show enhanced dielectric properties under a bias electric field,^{23,24} due to the gradient of their spontaneous polarization in the films, according to Mantese and colleagues.^{25–27} Accordingly, compositional-gradient BTS thin film is a promising candidate for tunable dielectric materials. This requires further study. Traditionally, thin films have been fabricated by magnetron sputtering, pulsed laser deposition, and sol-gel spinning coating. Sol-gel with spinning coating has the advantages of simple, repeatable and easily quality-controlled.

In this study, compositional-gradient BTS thin films are prepared by sol-gel together with spin coating. There is no need for compositional-gradient BTS thin films to operate under high tuning voltages, which can avoid safety hazards. It has been observed that compositional-gradient BTS thin

films simultaneously have a moderate dielectric constant, low dielectric loss, high tunability under low tuning voltage (where the tuning voltage is 8 V and the corresponding bias electric field is 16 kV/mm), and excellent temperature stability.

2. Experimental Procedures

2.1. Fabrication of BTS thin films

$\text{BaTi}_{1-x}\text{Sn}_x\text{O}_3$ (BTS) thin films are prepared using sol-gel and spin coating. A BTS precursor solution is prepared from barium acetate ($\text{Ba}(\text{CH}_3\text{COO})_2$), tin 2-ethylhexanoate ($\text{C}_{16}\text{H}_{30}\text{O}_4\text{Sn}$), and titanium *n*-butoxide ($\text{Ti}(\text{O}(\text{CH}_2)_3\text{CH}_3)_4$). Glacial acetic acid (CH_3COOH) and 2-methoxyethanol ($\text{CH}_3\text{OCH}_2\text{CH}_2\text{OH}$) are used as solvents, and acetylacetone (AcAc , $\text{CH}_3\text{COCH}_2\text{COCH}_3$) is used as polymerizing agents. First, titanium *n*-butoxide and acetylacetone are mixed at a predetermined ratio. Then 2-methoxyethanol is added and stirred continuously for 0.5 h. The molar ratios of Ti:AcAc and Ti:2-methoxyethanol are 1:2 and 1:5, respectively. Tin 2-ethylhexanoate is then added to the solution while stirring (solution 1). Second, barium acetate is dissolved in the acetic acid solution under stirring for 0.5 h (solution 2). Finally, solution 2 is mixed with solution 1, and glacial acetic acid is added to control the concentration of the final solution of the BTS precursor solution to 0.35 mol/L.

After aging for 24 h, the sol-gel thin films are deposited on Pt(100)/Ti/SiO₂/Si substrates by spin coating at a deposition rate of 3000 rpm and a deposition time of 30 s for each layer. The sol-gel deposited thin films are preheated in a tube furnace at 150 °C, 300 °C, and 450 °C for 5 min, at each temperature, to evaporate the solvents and decompose the organic residuals. The above process is repeated for five times to obtain the preheated thin films. Finally, the preheated thin films are annealed at 700 °C for 1 h to obtain the resulting thin films. In $\text{BaTi}_{1-x}\text{Sn}_x\text{O}_3$ thin films, $x = 0.1, 0.15, 0.2, 0.25,$ and 0.3 are denoted as BTS10, BTS15, BTS20, BTS25, and BTS30. In this paper, compositional-gradient BTS thin films are fabricated and denoted as BTS10/15/20, BTS15/20/25, and BTS20/25/30. The structures are illustrated in Fig. 1.

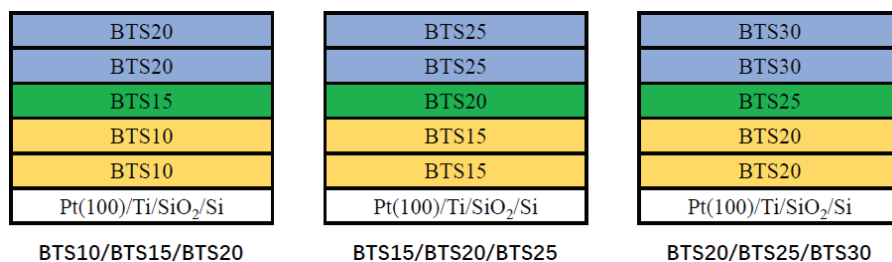


Fig. 1. Structure diagrams for BTS10/15/20, BTS15/20/25, and BTS20/25/30.

2.2. Characterization

To investigate whether there are elements of impurities in the thin films, the samples are analyzed with X-ray photoelectron Spectroscopy (XPS, Thermo Scientific K-Alpha, USA). The crystalline phase is characterized through grazing-incident X-ray diffraction (GIXRD, Bruker D8, Germany), using Cu $K\alpha$ radiation. The Raman spectra are acquired using a Raman scattering spectrometer (Raman, Horiba Evolution, France). To determine the surface morphology and thickness of thin films, samples are analyzed with scanning electron microscopy (SEM, SU8010, Japan). Gold electrodes with a 1 mm diameter are sputtered onto the surface of the thin films as the top electrodes for measuring dielectric properties. The temperature-dependent dielectric constant ($\epsilon-T$) curves are tested at the computer-controlled heating/cooling stage (INSTECH, USA). The frequency-dependent dielectric constant and dielectric loss are measured using IM3536 LCR Meter (HIOKI, Japan) from 10 KHz to 1 MHz at room temperature, and the leakage current density dependent on the bias electric field is identified with a voltage-current source (KEITHLEY 2400, America). In addition, dielectric tunable properties are tested with a Precision LCR Meter (TH2838H, China).

3. Results and Discussion

3.1. XPS analyses

Figure 2 illustrates the XPS survey of the compositional-gradient BTS thin films to confirm the presence of Ba, Sn, Ti, and O in the sample. The spectrum confirms the cleanliness of the compositional-gradient thin films, as no impurity peaks are found except for the peaks caused by C (carbon), which is adventitious.^{28,29} That is to say, the XPS results demonstrate

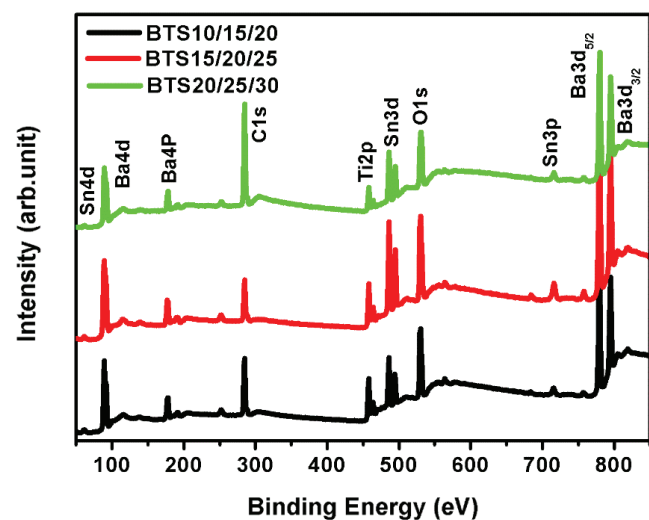


Fig. 2. XPS spectra of BTS10/15/20, BTS15/20/25, and BTS20/25/30.

the successful introduction of Ba, Sn, Ti, and O elements in the compositional-gradient BTS thin films and the cleanliness of the thin films.

3.2. XRD and Raman analyses

Figure 3(a) shows room temperature GIXRD patterns of compositional-gradient BTS thin films after annealing at 700 °C for 1 h. It is evident from the figure that all of the samples are crystallized into single-phase solid solutions of perovskite structure, as (100), (110), (111), (200), (210), and (211) peaks can clearly be observed.³⁰ No peak splitting of the perovskite structure can be seen, indicating a pseudo-cubic phase in the microstructure scale. However, because the resolution of the XRD results is limited, owing to the Lorentzian broadening

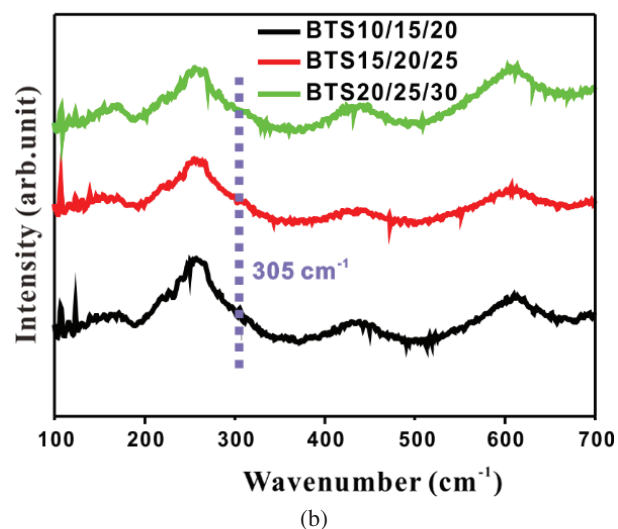
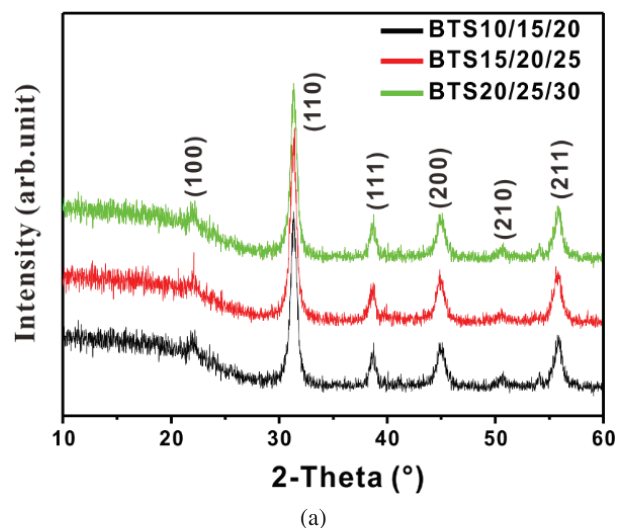


Fig. 3. (a) GIXRD patterns in the 2-Theta range of 10–60° and (b) Raman spectra of BTS10/15/20, BTS15/20/25, and BTS20/25/30.

of the reflections, the existence of tetragonal distortions cannot be excluded at the microscopic scale.³¹

Figure 3(b) shows the Raman spectra of compositional-gradient BTS thin films. Raman spectra can detect impurity phases at lower concentrations and are more sensitive to noncrystalline phases than XRD. The structural information from Raman spectra involves single TiO_6 octahedra. According to previous studies,^{32,33} the sharp “silent” mode at 305 cm^{-1} refers to the tetragonal phase. However, in this paper, this mode disappears in the compositional-gradient BTS thin films, and the Raman patterns are consistent with the cubic phase of BaTiO_3 . Hence, the results for GIXRD and Raman spectra support the crystallization state and pseudo-cubic phase in compositional-gradient BTS thin films.

3.3. SEM analyses

Generally speaking, a smooth, flat, and crack-free morphology grants excellent properties of thin films.³⁴ The surface morphology of thin films can greatly influence their properties. SEM micrographs of compositional-gradient BTS thin films are shown in Fig. 4. The results demonstrate that the surface morphology of BTS10/15/20, BTS15/20/25, and BTS20/25/30 thin films is dense, crack-free, and well-crystallized in granular grains with a uniform thickness of $\sim 500\text{ nm}$. The crystalline structure of thin films, as seen in the SEM results, is in good agreement with XRD analyses.

In addition, from the cross-sectional SEM image in Figs. 4(a₁), 4(b₁), and 4(c₁), a clear interface can be seen

between $\text{Pt}(100)/\text{Ti}/\text{SiO}_2/\text{Si}$ substrates and compositional-gradient BTS thin films, and no defects can be observed at the interface between substrates and thin films. It is also worth noting that no visible internal interface exists throughout the thickness of compositional-gradient BTS thin films, that is to say, there are no structurally visible internal interfaces that separate the individual layer compositions from one another. This is because BTS10, BTS15, BTS20, BTS25, and BTS30 thin films are similar and appear homogeneous in nature, hence lacking the structural interface of the internal compositional layers.³⁵

3.4. Dielectric properties

The temperature dependence of the dielectric constant and dielectric loss of BTS10/15/20, BTS15/20/25, and BTS20/25/30 measured at 1 MHz from -95°C to 150°C are shown in Figs. 5(a) and 5(b). The dielectric constant of compositional-gradient BTS thin films is generally depressed compared to single BTS thin films (Fig. 6), which facilitates their application in tunable components and devices when impedance matching in circuits is taken into account. When two layers with different polarizations are connected, the polarizations can cause difference in performance at the interface, so the dielectric constant of the compositional-gradient BTS thin films is generally suppressed.

It can also be noted that the dielectric constant exhibits dispersion as a function of temperature, which means that compositional-gradient BTS thin films possess a broader,

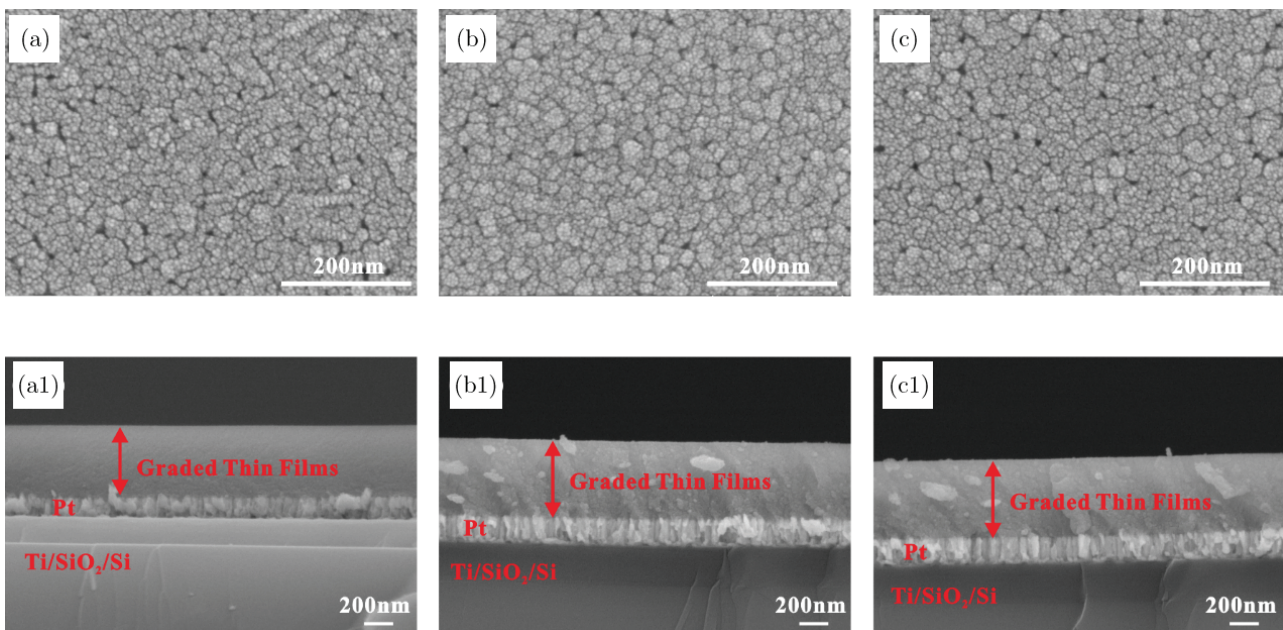


Fig. 4. SEM images of (a) BTS10/15/20, (b) BTS15/20/25, (c) BTS20/25/30 and cross-sectional SEM images of (a₁) BTS10/15/20, (b₁) BTS15/20/25, (c₁) BTS20/25/30.

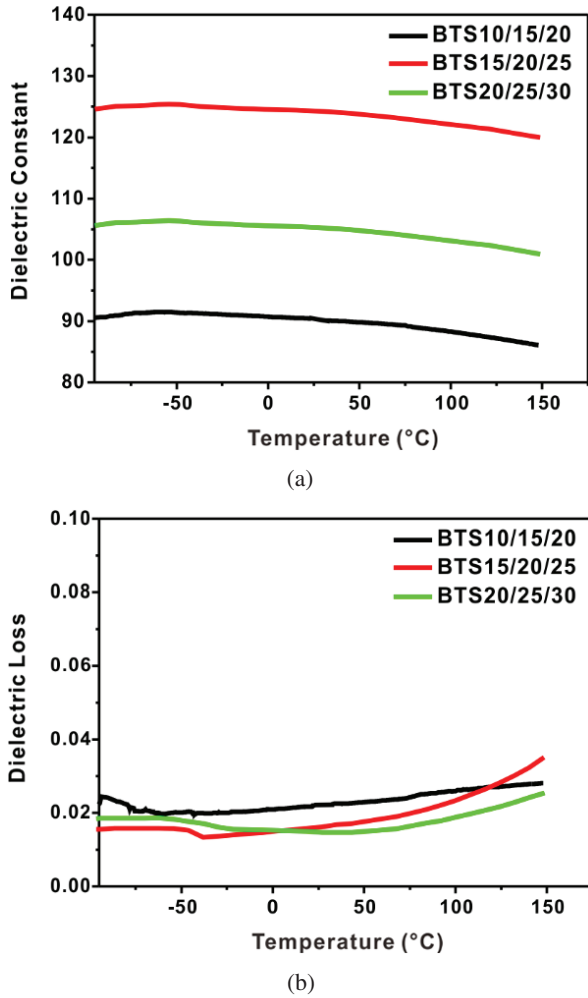


Fig. 5. Temperature-dependent (a) dielectric constant and (b) dielectric loss of BTS10/15/20, BTS15/20/25, and BTS20/25/30.

flatter, and diffused dielectric response with change in temperature, thus reducing the dependence of dielectric behaviors on temperature. It was shown in a theoretical study that the temperature sensitivity of dielectric response in the gradient structure can be tailored by adjusting the degree of compositional variation.³⁶ The TCC is used to evaluate the temperature stability³⁷:

$$TCC = \Delta C / (C_0 \Delta T), \quad (3)$$

where ΔC is the change in capacitance with respect to C_0 at 20°C, and ΔT is the change in temperature with respect to 20°C. The TCC values are calculated with Eq. (3) and are displayed in Table 1, where it can be seen that the TCC_{20-150} and $TCC_{20-(-95)}$ values are only $-0.9 \times 10^{-4}/^\circ\text{C}$ and $-3.8 \times 10^{-4}/^\circ\text{C}$ for BTS10/15/20 thin film. The low TCC value indicates temperature stability, which is important for tunable components and devices that operate over a wide range of temperatures near room temperature. Although the reason for low TCC values is not clear, it is believed that the preparation method, the composition, the substrate type, the electrode type, the annealing temperature, the defects, and the microstructure of compositional-gradient BTS thin films all play a significant role in temperature stability.³⁸ According to Cole and colleagues, the diffusion of dielectric response with the temperature can be attributed to the polarization grading and interlayer interactions in compositional-gradient thin films.³⁵

Figure 7(a) exhibits the dielectric response of BTS10/15/20, BTS15/20/25, and BTS20/25/30 as a function of frequency. The dielectric constant of compositional-gradient BTS thin films is lower than that of single BTS thin films (Fig. 6) and the dielectric constant of BTS10/15/20 is 111 at 1 MHz. This is due to interface differences caused by gradient polarization, as described above. In addition, the

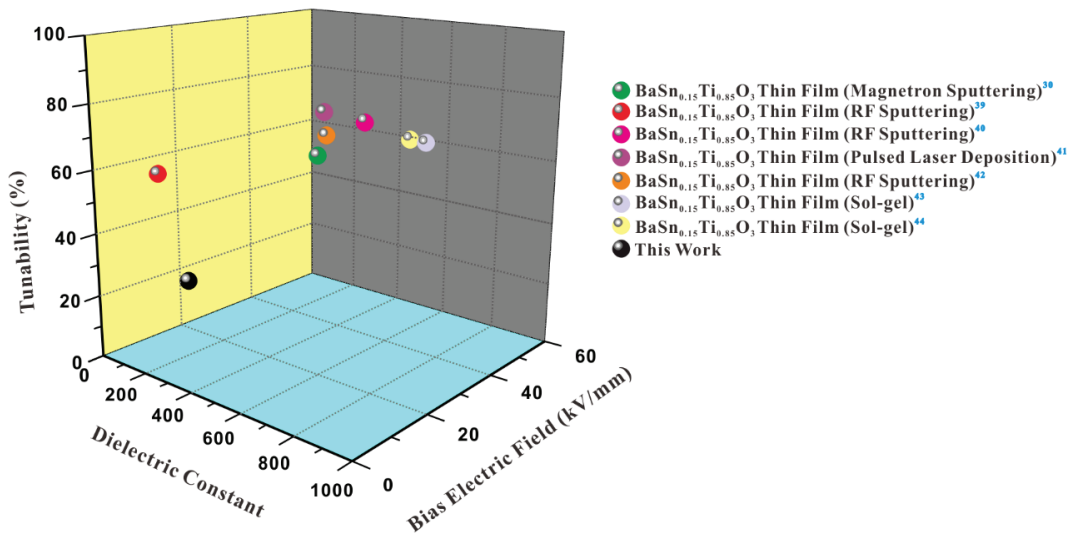


Fig. 6. Comparison of maximum dielectric constant, tunability, and bias electric field between compositional-gradient BTS thin films and single BTS thin films.

Table 1. Comparison of the values of the temperature coefficient of capacitance (TCC) with respect to 20 °C for BTS10/15/20, BTS15/20/25, and BTS20/25/30.

Sample	TCC ₂₀₋₁₅₀ (10 ⁻⁴ /°C)	TCC _{20-(−95)} (10 ⁻⁴ /°C)
BTS10/15/20	−0.9	−3.8
BTS15/20/25	−0.6	−2.8
BTS20/25/30	−0.7	−3.3

increasing trend of dielectric loss before 1 MHz may be due to the influence of contact resistance of the probe and electrode and the LC resonance caused by the lead wire and the tested film capacitor.⁴⁴

The leakage current density of compositional-gradient BTS thin films as a function of the bias electric field is shown in Fig.7(b). This indicates that the leakage current density of compositional- gradient BTS thin films is low at 16 kV/mm, and in BTS10/15/20, the leakage current density is 7.4×10^{-7} A/cm². This may be due to defects, for instance, charge carriers, being trapped at compositional interfaces, which can build barriers to depress defect movement.⁴⁵ The reduction in the dielectric constant and leakage current density is of great importance for electrically tunable components and devices.

The variation range of the dielectric constant under the bias electric field is an important indicator for dielectric tunable materials. The bias electric field dependent dielectric constant for BTS10/15/20, BTS15/20/25, and BTS20/25/30 is presented in Fig. 8(a). Dielectric tunability is calculated by the dielectric constant in Fig. 8(a) according to Eq. (1) and is shown in Fig. 8(b). As expected, for all thin films, tunability increases with increasing bias electric field. The tunability of BTS10/15/20, BTS15/20/25, and BTS20/25/30 is 20.1%, 16.1%, and 17.2% at 1 MHz under 16 kV/mm, respectively.

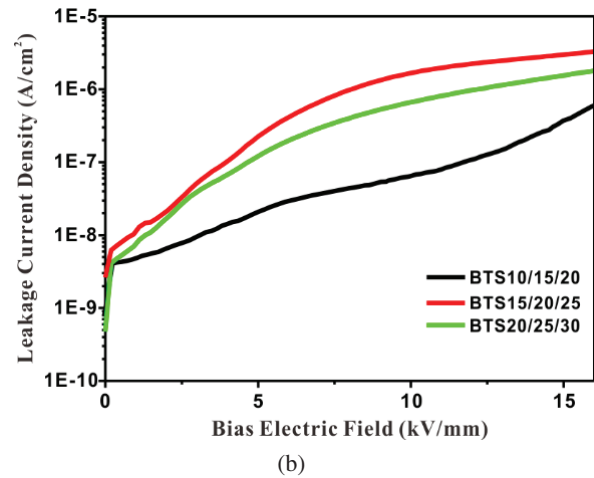
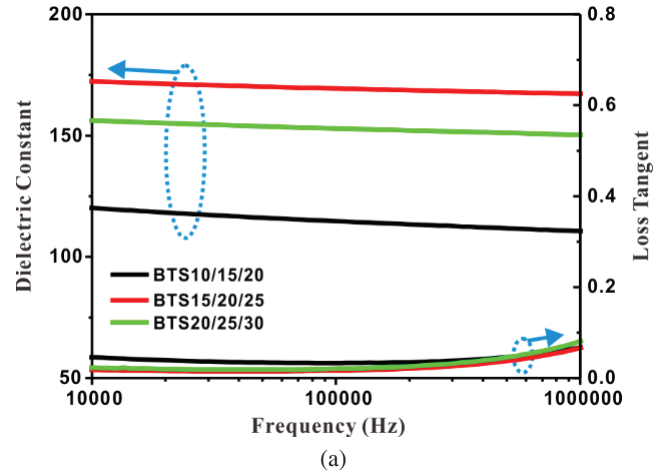


Fig. 7. (a) Dielectric constant and dielectric loss of BTS10/15/20, BTS15/20/25, and BTS20/25/30 as a function of frequency; (b) leakage current density of BTS10/15/20, BTS15/20/25, and BTS20/25/30 as a function of bias electric field.

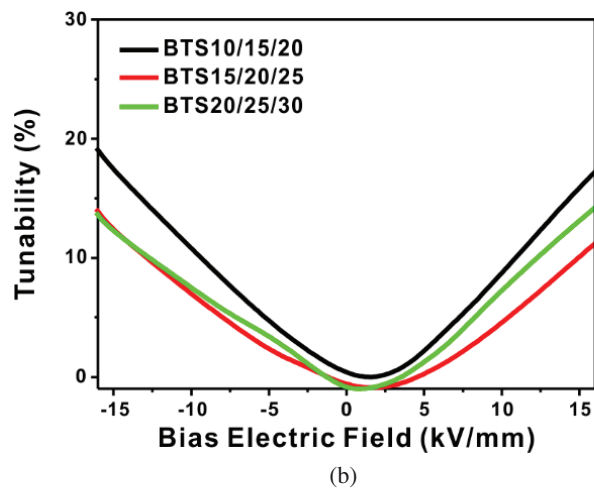
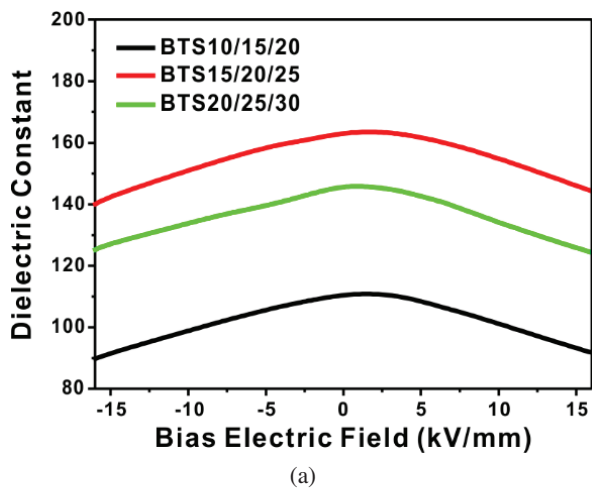


Fig. 8. (a) Dielectric constant, (b) dielectric tunability, (c) dielectric loss for BTS10/15/20, BTS15/20/25, and BTS20/25/30 as a function of the bias electric field at 1 MHz; (d) dielectric tunability and FOM values of BTS10/15/20, BTS15/20/25, and BTS20/25/30 at 1 MHz under 16 kV/mm.

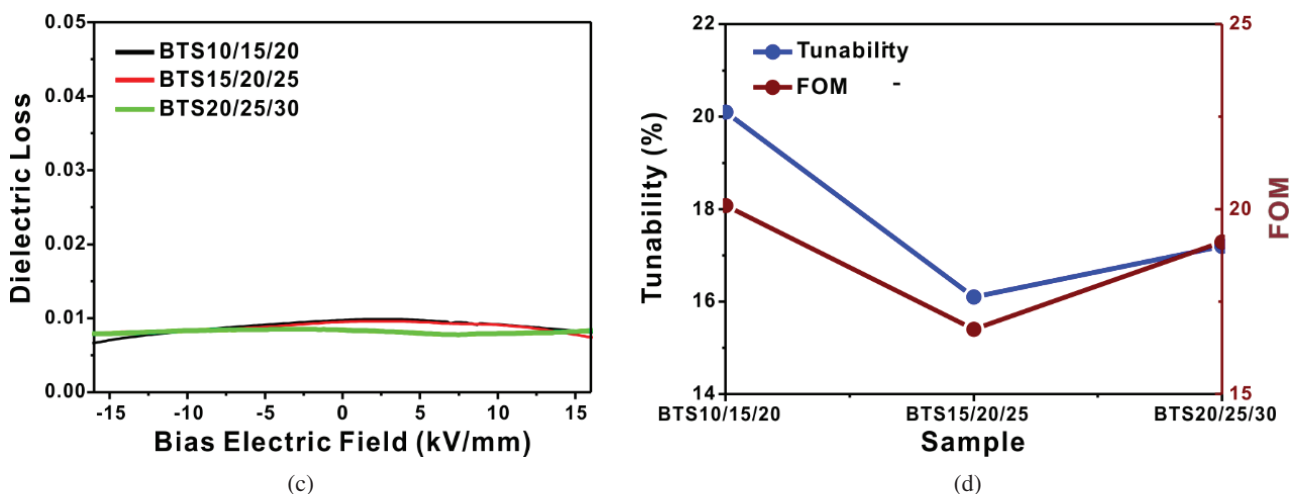


Fig. 8. (Continued)

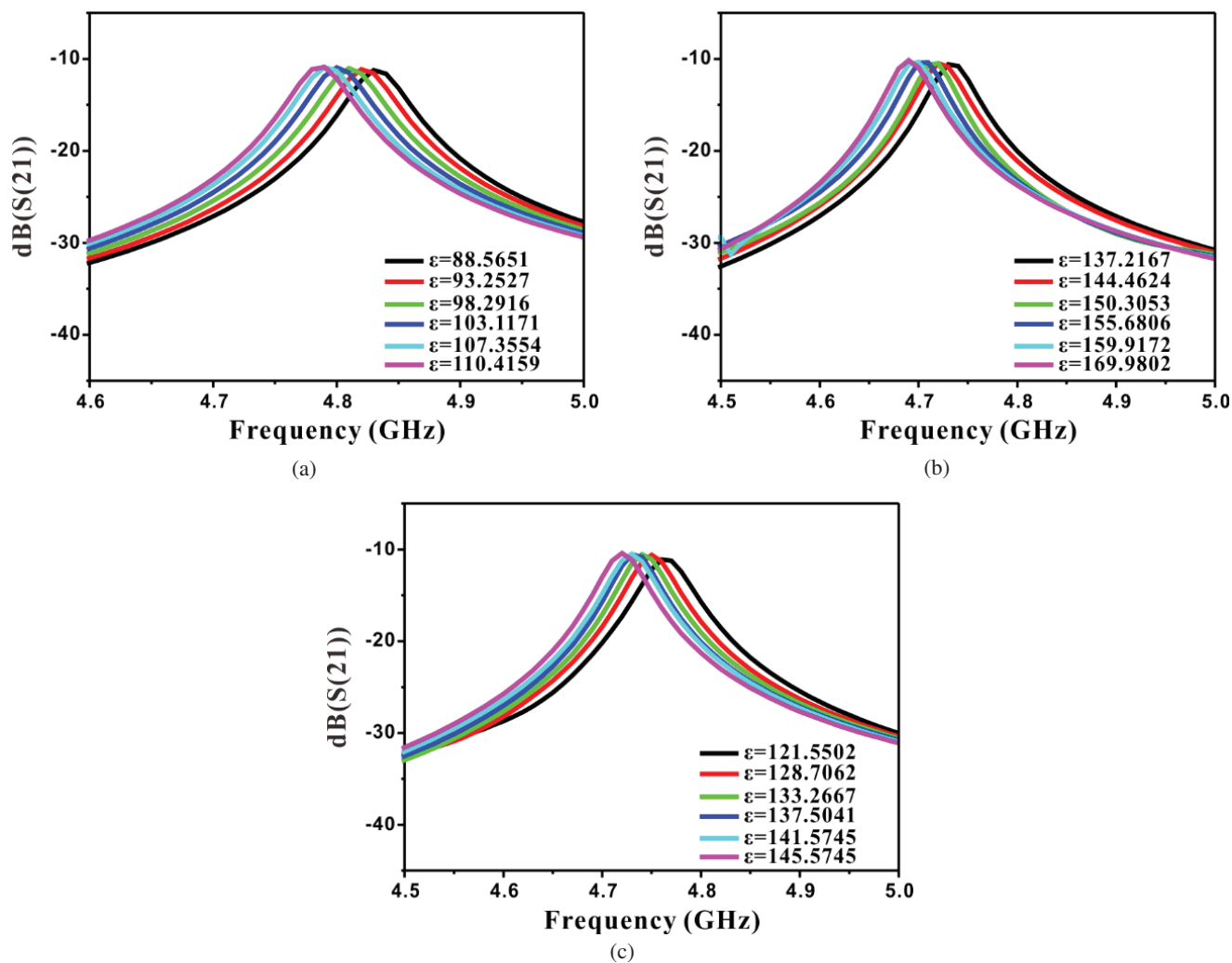


Fig. 9. Simulation results for transmission response (S(21)) as a function of frequency for (a) BTS10/15/20; (b) BTS15/20/25, and (c) BTS20/25/30.

Although the tunability of compositional-gradient BTS thin films decreases with comparison to single BTS thin films as a result of reduced dielectric constant (Fig. 6), it retains significant tunability under low bias electric field, which avoids the high tuning voltage, as described above.

Figure 8(c) shows the dielectric loss dependent on the bias electric field of compositional-gradient BTS thin films. The maximum dielectric loss for BTS10/15/20, BTS15/20/25, and BTS20/25/30 is 0.00988, 0.00961, and 0.00851, respectively. Low dielectric loss can result from the fact that defects within thin films are trapped at the compositional interface and can no longer move to compensate for the polarization difference between layers.⁴⁵ Therefore, the trapped defects do not reach to the electrodes, promoting the enhanced dielectric characteristics of compositional-gradient BTS thin films.

The FOM value shown in Fig. 8(d) is introduced to evaluate the comprehensive tunable properties of compositional-gradient BTS thin films. The FOM value of BTS10/15/20, BTS15/20/25, and BTS20/25/30 is 20.10, 16.75, and 19.11, respectively. It is worth noting that the BTS10/15/20 shows the largest FOM value due to its high tunability and low dielectric loss.

The above discussion indicates that compositional-gradient thin films, particularly for BTS10/15/20, show great benefits, in terms of excellent temperature stability ($TCC_{20-150} = -0.9 \times 10^{-4}/^{\circ}\text{C}$), decreased dielectric constant (88–111), low loss tangent (0.00988), low leakage current density ($7.4 \times 10^{-7} \text{ A/cm}^2$), and high tunability (20.1%) under low tuning voltage (8 V, where the corresponding bias electric field is 16 kV/mm).

Figure 9 presents the simulation response for transmission response $S(21)$ as a function of frequency after applying a variable bias electric field to the compositional-gradient BTS thin films. $S(21)$ describes the voltage transmission coefficient from the first port to the second when the second port is connected to a matching load. For BTS10/15/20, when dielectric constant is 110.4159 under a 0 kV/mm bias, the resonant frequency is 4.79 GHz and finally moves to 4.83 GHz when dielectric constant is 88.5651 under a 16 kV/mm bias, as seen in Fig. 9(a). At the same time, when the bias electric field is between 0 kV/mm and 16 kV/mm, the resonant frequency of BTS15/20/25 [Fig. 9(b)] and BTS20/25/30 [Fig. 9(c)] moves from 4.69 GHz to 4.73 GHz and 4.72 GHz to 4.76 GHz, respectively. The simulated resonant frequency for compositional-gradient BTS thin films depends on the bias electric field, showing that thin films could be used in electrically controllable and frequency selective tunable components and devices.⁶

4. Conclusion

In summary, compositional-gradient BTS thin films are deposited on Pt(100)/Ti/SiO₂/Si substrates with sol-gel using spin coating. The thin films have a crystallization structure with a crack-free and dense morphology consisting of a

pseudo-cubic phase. For BTS10/15/20 thin films, the TCC_{20-150} and $TCC_{20-(95)}$ value is only $-0.9 \times 10^{-4}/^{\circ}\text{C}$ and $-3.8 \times 10^{-4}/^{\circ}\text{C}$, respectively, demonstrating high temperature stability. The results also show that the thin films exhibit low leakage current density and low dielectric loss due to the defects trapped at their interfaces and do not reach the electrode. At the same time, the tunability is 20.1% under 16 kV/mm at 1 MHz for BTS10/15/20 thin films, while the dielectric constant ranges from 88 to 111. The obtained tunability for compositional-gradient BTS thin films avoids the use of high tuning voltages, and the moderate dielectric constant is beneficial for impedance matching in circuits. In addition, the simulated resonant frequency for compositional-gradient BTS thin films depends on the bias electric field, as can be seen from the simulation results, which means that the thin films can be used in electrically tunable applications. These excellent properties make compositional-gradient BTS thin films a promising candidate to be used in tunable components and devices.

Author Contributions

Chenjing Wu: Methodology, Investigation, Validation, Formal analyses, Writing-Original draft.

Manwen Yao: Conceptualization, Supervision, Project administration, Funding acquisition.

Conflicts of interest

The authors declare that they have no known competing financial interests or personal relations that could have appeared to influence the work reported in this paper.

Acknowledgments

This work was supported by the Joint Fund of the Ministry of Education of China under the grant number 6141A02022433.

References

- B. Luo, Y. W. Xu, Y. W. Xu, F. Z. Zhang, T. T. Wang and Y. B. Yao, Dielectric tunability properties in (110)-oriented epitaxial $0.5\text{Ba}(\text{Ti}_{0.8}\text{Zr}_{0.2})-0.5(\text{Ba}_{0.7}\text{Ca}_{0.3})\text{TiO}_3$ thin films prepared by PLD method, *Materials* **13**, 4772 (2020).
- H. Zaitouni, L. Hajji, D. Mezzane, E. Choukri, Y. Gagou, K. Houmada, A. Charia, A. Alimoussa, B. Rozic, M. E. Marssi and Z. Kutnjak, Structural, dielectric, ferroelectric and tuning properties of Pb-free ferroelectric $\text{Ba}_{0.9}\text{Sr}_{0.1}\text{Ti}_{1-x}\text{Sn}_x\text{O}_3$, *Ceram. Int.* **46**, 27275 (2020).
- C. Borderon, S. Ginestar, H. W. Gundel, A. Haskou, K. Nadaud, R. Renoud and A. Sharaiha, Design and development of a tunable ferroelectric microwave surface mounted device, *IEEE. Trans. Ultrason. Ferr.* **67**, 1733 (2020).
- Z. H. Tang, Z. S. Jiang, D. J. Lei, J. Q. Huang, F. Qiu, Y. Q. Chen, H. M. Deng and M. Yao, An electro-optic tunable microwave delay-line using the piezoelectric-piezomagnetic superlattices with an external DC electric field, *Phys. Lett. A* **385**, 126962 (2021).

- ⁵L. Curecheriu, V. A. Lukacs, L. Padurariu, G. Stoian and C. E. Ciomaga, Effect of porosity on functional properties of lead-free piezoelectric BaZr_{0.15}Ti_{0.85}O₃ porous ceramics, *Materials* **13**, 3324 (2020).
- ⁶H. F. Zhang, H. Giddens, Y. J. Yue, X. Z. Xu, V. A. Peters, V. Koval, M. Palma, I. Abrahams, H. X. Yan and Y. Hao, Polar nano-clusters in nominally paraelectric ceramics demonstrating high microwave tunability for wireless communication, *J. Eur. Ceram. Soc.* **40**, 3996 (2020).
- ⁷S. Sharma, J. M. Siqueiros and O. R. Herrera, Structural, dielectric, ferroelectric and optical properties of Er doped BiFeO₃ nanoparticles, *J. Alloy. Compd.* **853**, 156979 (2021).
- ⁸A. Mostaed, I. Bakaimi, B. Hayden, D. C. Sinclair and I. M. Reaney, Origin of improved tunability and loss in N₂ annealed barium strontium titanate films, *Phys. Rev. Mater.* **4**, 094410 (2020).
- ⁹C. Cochard, T. Spielmann and T. Granzow, Dielectric tunability of ferroelectric barium titanate at millimeter-wave frequency, *Phys. Rev. B* **100**, 184104 (2019).
- ¹⁰L. L. Gendre, C. L. Paven, M. Haydoura, R. Benzerga, F. Marlec, A. Sharaiha, F. Chevre, F. Tessier and A. Moreaac, Thermal oxidation of oxynitride films as a strategy to achieve (Sr₂Ta₂O₇)_{100-x}(La₂Ti₂O₇)_x based oxide perovskite films with $x = 1.65$, *J. Eur. Ceram. Soc.* **40**, 6293 (2021).
- ¹¹P. M. Vilarinho, Z. Fu, A. I. Kingon and A. Tkach, Low loss tunable dielectric BaNd₂Ti₅O₁₄-(Ba_{0.5}Sr_{0.5})TiO₃ composite thick films, *Scr. Mater.* **155**, 160 (2018).
- ¹²H. T. Dong, J. Jian, H. F. Li, D. R. Jin, J. G. Chen and J. R. Cheng, Improved dielectric tunability of PZT/BST multilayer thin films on Ti substrates, *J. Alloy. Compd.* **725**, 54 (2017).
- ¹³H. T. Dong, H. F. Li, J. G. Chen, D. R. Jin and J. R. Chen, Investigation of the effects of misfit strain on barium strontium titanate thin films deposited on base metal substrates by a modified phenomenological model, *J. Appl. Phys.* **122**, 144104 (2017).
- ¹⁴R. D. Richtmyer, Dielectric resonators, *J. Appl. Phys.* **10**, 391 (1939).
- ¹⁵S. P. Wang, K. Hu, F. Huang, M. Zhang, S. Wu, Q. C. Liu and X. K. Kong, Activating microwave absorption via noncovalent interactions at the interface based on metal-free graphene nanosheets, *Carbon* **152**, 818 (2019).
- ¹⁶M. M. Hossen, S. Nasrin and M. B. Hossen, Effect of Mn²⁺ doping on structural, magnetic and electrical properties of Ni_{0.5-x}Mn_xCu_{0.2}Cd_{0.3}Fe₂O₄ nano ferrites prepared by sol-gel auto combustion method for high-frequency applications, *Physica B* **599**, 412456 (2019).
- ¹⁷T. Teranishi, R. Kanemoto, H. Hayashi and A. Kishimoto, Effect of the (Ba+Sr)/Ti ratio on the microwave-tunable properties of Ba_{0.6}Sr_{0.4}TiO₃ ceramics, *J. Am. Ceram. Soc.* **100**, 1037 (2017).
- ¹⁸S. Patel, A. Chuauhan, R. Vaish and P. Thomas, Enhanced energy storage performance of glass added 0.71Bi_{0.52}Na_{0.5}TiO₃-0.065BaTiO₃-0.33SrTiO₃ ferroelectric ceramics, *J. Asian. Ceram. Soc.* **3**, 383 (2015).
- ¹⁹A. Saeed, B. Ruthramurthy, W. H. Yong, O. B. Hoong, T. K. Ban and Y. H. Kwang, Structural and dielectric properties of substituted barium titanate ceramics for capacitor applications, *Ceram. Int.* **41**, 13425 (2015).
- ²⁰X. L. Chen, J. Chen, G. S. Huang, D. D. Ma, L. Fang and H. F. Zhou, Relax or behavior and dielectric properties of Bi(Zn_{2/3}Nb_{1/3})O₃-modified BaTiO₃ ceramics, *J. Electron. Mater.* **44**, 4804 (2015).
- ²¹Y. R. Wang, Y. P. Pu and P. P. Zhang, Investigation of dielectric relaxation in BaTiO₃ ceramics modified with BiYO₃ by impedance spectroscopy, *J. Alloy. Compd.* **653**, 596 (2015).
- ²²V. V. Shvartsman and D. C. Lupascu, Lead-free relaxor ferroelectrics, *J. Am. Ceram. Soc.* **95**, 1 (2012).
- ²³S. U. Adikary and H. L. W. Chan, Compositionally graded Ba_xSr_{1-x}TiO₃ thin films for tunable microwave applications, *Mater. Chem. Phys.* **79**, 157 (2003).
- ²⁴P. R. Ren, Y. K. Sun, X. Wang, H. Q. Fan and G. Y. Zhao, Dielectric properties of compositionally graded Ba_{1-x}La_xTi_{1-x/4}O₃ thick films, *Ceram. Int.* **43**, 5347 (2017).
- ²⁵S. Zhong, Z. G. Ban, S. P. Alpay and J. V. Mantese, Large piezoelectric strains from polarization graded ferroelectrics, *Appl. Phys. Lett.* **89**, 142913 (2006).
- ²⁶J. V. Mantese, N. W. Schubring, A. L. Michell, A. B. Catalan, M. S. Mohammed, R. Naik and G. W. Auner, Slater model applied to polarization graded ferroelectrics, *Appl. Phys. Lett.* **71**, 2047 (1997).
- ²⁷M. S. Mohammed, G. W. Auner, R. Naik, J. V. Mantese, N. W. Schubring, A. L. Michell and A. B. Catalan, Temperature dependence of conventional and effective pyroelectric coefficients for compositionally graded Ba_xSr_{1-x}TiO₃ films, *J. Appl. Phys.* **84**, 3322 (1998).
- ²⁸S. M. D. Watson, K. S. Coleman and A. K. Chakraborty, A new route to the production and nanoscale patterning of highly smooth, ultrathin zirconium oxide films, *ACS Nano* **2**, 643 (2008).
- ²⁹Y. V. Butenko, S. Krishnamurthy, A. K. Chakraborty, V. L. Kuznetsov, V. R. Dhanak, M. R. C. Hunt and L. Siller, Photoemission study of onionlike carbons produced by annealing nanodiamonds, *Phys. Rev. B* **71**, 075420 (2005).
- ³⁰M. Y. Wu, C. M. Zhang, S. H. Yu and L. X. Li, Effect of sputtering pressure on structural and dielectric tunable properties of BaSn_{0.15}Ti_{0.85}O₃ thin films grown by magnetron sputtering, *Ceram. Int.* **44**, 10236 (2018).
- ³¹S. T. Zhang, A. B. Kounga and E. Aulbach, Giant strain in lead-free piezoceramics Bi_{0.5}Na_{0.5}TiO₃-BaTiO₃-K_{0.5}Na_{0.5}NbO₃ system, *Appl. Phys. Lett.* **91**, 112906 (2007).
- ³²M. J. Ansaree, U. Kumar and S. Upadhyay, Solid-state synthesis of nano-sized Ba(Ti_{1-x}Sn_x)O₃ powders and dielectric properties of corresponding ceramics, *Appl. Phys. A-Mater.* **123**, 432 (2017).
- ³³C. J. Xiao, C. Q. Jin and X. H. Wang, Crystal structure of dense nanocrystalline BaTiO₃ ceramics, *Mater. Chem. Phys.* **111**, 209 (2008).
- ³⁴S. H. Yu, W. T. Lou, C. M. Zhang, M. Y. Wu, L. J. Ge, H. L. Dong and L. X. Li, (110)-textured Ba(Sn_{0.15}Ti_{0.85})O₃/Ba_{0.6}Sr_{0.4}TiO₃/BaZr_{0.2}Ti_{0.8}O₃ multilayers with enhanced tunable performance, *J. Alloy. Compd.* **781**, 689 (2019).
- ³⁵M. W. Cole, E. Ngo, S. Hirsch and J. D. Demaree, The fabrication and material properties of compositionally multilayered Ba_{1-x}Sr_xTiO₃ thin films for realization of temperature insensitive tunable phase shifter devices, *J. Appl. Phys.* **102**, 034104 (2007).
- ³⁶Z. G. Ban, S. P. Alpay and J. V. Mantese, Hysteresis offset and dielectric response of compositionally graded ferroelectric materials, *Integr. Ferroelectr.* **58**, 1281 (2003).
- ³⁷S. Y. Lee and K. W. Paik, Reduced temperature coefficient capacitance (TCC) of embedded capacitor films (ECFs) for organic substrates using SrTiO₃ and multifunctional epoxy, *J. Electron. Mater.* **39**, 1358 (2010).
- ³⁸M. W. Cole, C. Hubbard, E. Ngo, M. Ervin and M. Wood, Structure-property relationships in pure and acceptor-doped Ba_{1-x}Sr_xTiO₃ thin films for tunable microwave device applications, *J. Appl. Phys.* **92**, 475 (2002).
- ³⁹G. S. Zhu, D. L. Yan, H. R. Xu and A. B. Yu, Structural and electric properties of BaSn_{0.15}Ti_{0.15}O₃ thin films on ITO/glass substrate by RF sputtering from powder target, *Mater. Lett.* **140**, 155 (2015).
- ⁴⁰M. Y. Wu, X. P. Li, H. L. Dong, S. H. Yu and L. X. Li, High-performance flexible dielectric tunable BTS thin films prepared on copper foils, *Ceram. Int.* **45**, 16270 (2019).
- ⁴¹M. Y. Wu, S. H. Yu, L. He, L. Yang and W. F. Zhang, Influence of oxygen pressure on microstructure and dielectric properties of lead-free BaSn_{0.15}Ti_{0.15}O₃ thin films prepared by pulsed laser deposition, *Ceram. Int.* **42**, 15793 (2016).

⁴²M. Y. Wu, C. M. Zhang, S. H. Yu and L. X. Li, Thickness dependence of microstructure, dielectric and leakage properties of BaSn_{0.15}Ti_{0.15}O₃ thin films, *Ceram. Int.* **44**, 11466 (2018).

⁴³L. N. Gao, J. W. Zhai, S. N. Song and X. Yao, Crystal orientation dependence of the out-of-plane dielectric properties for barium stannate titanate thin films, *Mater. Chem. Phys.* **124**, 192 (2010).

⁴⁴M. Mascot, D. Fasquelle and J. C. Carru, Very high tunability of BaSn_xTi_{1-x}O₃ ferroelectric thin films deposited by sol-gel, *Funct. Mater. Lett.* **4**, 49 (2011).

⁴⁵A. L. Roytburd, S. F. Zhong and S. P. Alpay, Dielectric anomaly due to electrostatic coupling in ferroelectric-paraelectric bilayers and multilayers, *Appl. Phys. Lett.* **87**, 092902 (2005).